found that the dewatering time for the 1%, 2%, 3%, and 5% fly ash/fiber combinations was slower than the polymer conditioned only samples. It is believed that at low fibers percentage (1-5%), there are not enough fibers to change filter cake properties. At 10 % G-Nano concentration, the amount of fibers were enough to allow for more open structure of the fly ash filter cake, thus decreasing the dewatering time. For this type of fibers waste, therefore, a 10% concentration is the minimum amount required to show improvement in dewatering performance.

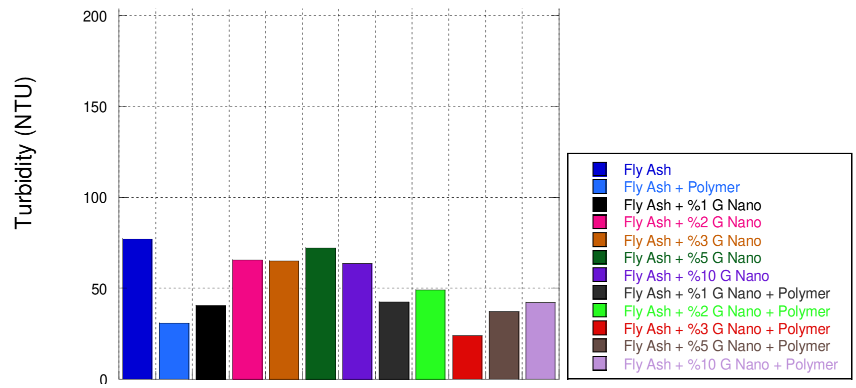

FIG. 6. Turbidity results for the fiber percentages with and without polymer.

In addition to measuring effluent volume in PFT test, the turbidity of the effluent that is collected in the graduated cylinder was also measured at the end of the test. Figure 6 shows the effluent turbidity for all the tested combinations. The turbidity values of the effluents were always less than 70 NTU for all cases and were generally lower than that of the fly ash alone. Notably increasing fiber percentage increases the turbidity slightly. It was also found that the polymer conditioned fly ash tests has the lowest turbidities. Minimum turbidity of 20 NTU was obtained for the 3% fiber with polymer samples.

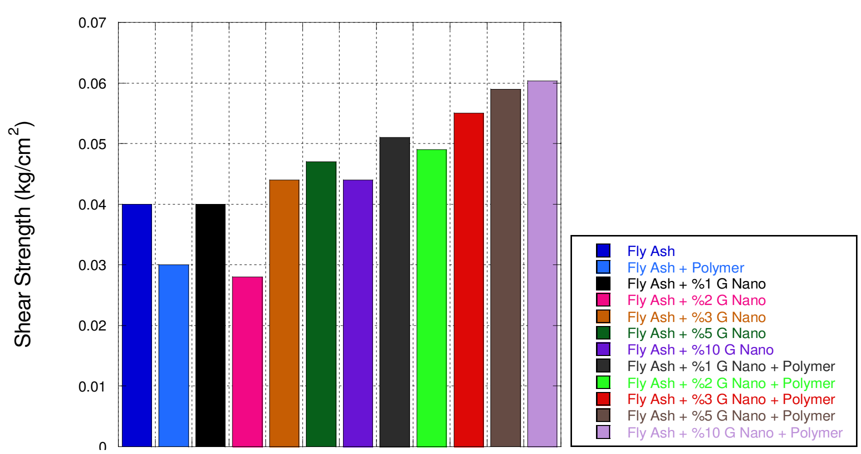

FIG. 7. Shear strength of the filter cake with and without fibers and polymer.

The effect of G-Nano waste on the shear strength of the filter cake is shown in Figure 7. The undrained shear strength of the filter cakes with different percentages of the fiber and/or polymer was determined. Generally, the shear strength of the filter cake increased with the increase of the fibers concentration. The maximum increase in strength was observed for the fly ash that is conditioned with polymer and mixed with the fiber. The shear strength of fly ash filter cake with 10% fiber and polymer was almost 150 % higher than that with no polymer. This is due to the increased interaction between the flocculated fly ash and the fibers.

Therefore, the current study results has proved that mixing fly ash with a fibrous materials, or with low percetage of fibers, allows for improvements in the dewatering rate of the fly ash, and increases the strength of the filter cake inside the geotextile tube. The future work in this area includes studying the effect of several fiber types on the dewtering rate and strength of fly ash filter cakes.

CONCLUSIONS

The effects of the anionic polymer flocculants and randomly dispersed fiber on dewatering performance and filter cake properties were investigated. Findings of this study are as follows:

1. Anionic flocculant increased dewatering rate but did not increase the shear strength of filter cake. Additionally, anionic polymers allowed for improvement in effluent turbidity.
2. Increasing G-Nano fiber percentage without polymer slightly improved the dewatering performance. Dewatering performance of fly ash that was mixed with polymer only is better than fly ash/polymer/fiber combinations except for 10% fiber/polymer mixture which yielded the best dewatering performance.
3. Fiber reinforcement increased the shear strength of the fly ash filter cakes. The shear strength increased by approximately 150 % when using fly ash that is conditioned with polymer and mixed with 10% G-Nano fibers.
4. Based on the results of this study, it can be concluded that the use of G-Nano waste yielded some improvement in dewatering time and in filter cake shear strength. It is believed that the use other waste types with higher percentages of fibers have the potential to improve the dewatering time and strength of the filter cake which is an important factor in the stacking of geotextile tubes.

ACKNOWLEDGEMENTS

The authors would like to thank the Higher Education Board of Turkey (YOK) for giving the first two authors the opportunity to participate in the YOK

Fellowship Program. The authors would like also to thank the National Science Foundation (NSF) (CMMI 1100131) and Geosynthetic Institute (GSI) for their support for this study.

REFERENCES

Ahmaruzzaman, M. (2010). ‘‘A review on the utilization of fly ash.’’ *Progress in Energy and Combustion Science*. 36: 327-363.

Davydov, M.V. (2012). “Stable operation of the water-slurry system at enrichment facilities.” *Coke and Chemistry*. 55(6): 197-203.

Grzelak, M.D., Maurer, B.W., Pullen, T.S., Bhatia, S.K., and Ramarao, B.V. (2011). ‘‘A comparison of test methods adopted for assessing geotextile tube dewatering performance.’’ *Proceedings of geo-frontiers*, Dallas, TX, USA: 2141-2151.

Heidrich, C., Feuerborn, H., and Weir, A. (2013). “Coal Combustion Products: a Global Perspective.” *Proc. of World of Coal Ash Conference (WOCA)*, Lexington, KY, USA.

Khachan, M.M., Bhatia, S.K., and Gustafson, A.C. (2012). ‘‘Dewatering and utilization of fly ash slurries using geotextile tubes.’’ *Indian Geotechnical Journal*. 42(3):194-205.

Koerner, G.R., and Koerner, R.M. (2006). ‘‘Geotextile tube assessment using a hanging bag test.’’ *Geotextiles and Geomembranes*. 24(2): 129-137.

Lawson,C.R. (2006). ‘‘Geotextile containment for hydraulic and environmental engineering.’’ *Geosynthetics International*. 15(6): 384-427.

Liao, K. and Bhatia, S.K. (2006). ‘‘Evaluation on filtration performance of woven geotextiles by falling head, pressure filtration test, and hanging bag tests.’’ *Proc. of 8th International Conference on Geosynthetics,* (CD-ROM), Yokohama Japan.

Lin, Y.K. (1971). ‘‘Compressibility, strength, and frost susceptibility of compacted fly ash.’’ *Ph.D Thesis*, Univeristy of Michigan, Michigan.

Maurer, B.W., Gustafson, A.C., Bhatia, S.K., and Palomino, A.M. (2012). ‘‘Geotextile dewatering of flocculated fiber reinforced fly-ash slurry.’’ *Fuel*. 97:411-417.

Muthukumaran, A.E., and Ilamparuthi, K. (2006). ‘‘Laboratory studies on geotextile filters as used in geotextile tube dewatering.’’ *Geotextiles and Geomembranes*. 24: 210–219.

Panday, K.K., Prasad, G., and Singh, V.N. (1985). ‘‘Copper(II) removal from aqueous solutions by fly ash.’’ *Water Research*. 19:869–873.

Ravina, D., and Mehta, P.K. (1986). ‘‘Properties of fresh concrete containing large amounts of fly ash.’’ *Cement and Concrete Research*. 16: 227-238.

Rao, M., Parwate, A.V., and Bhole, A.G. (2002). ‘‘Removal of Cr^{6+} and Ni^{2+} from aqueous solution using bagasse and fly ash.’’ *Waste Management*. 22:821–830.

Sridharan, A., and Prakash, K. (2010). ‘‘Coal ash utilization and sustainable waste management.’’ *The First US-India Workshop on Global Environmental Engineering Challenges*, New Delhi, India, 1-5.

Tang, Z., Ma, S., Ding, J., Wang, Y., Zheng, S., and Zhai, G. (2013). “Current Status and Prospect of Fly Ash Utilization in China.” *Proc. of World of Coal Ash Conference (WOCA)*, Lexington, KY, USA: 1-7.

Reliability Analysis of Monopile for Offshore Wind Foundation Using the Response Surface Method

G. L. Yoon[1], M.ASCE, S. B. Kim[2], and H. Y. Kim[3]

[1]Principal Researcher, Coastal Engineering & Ocean Energy Research Dept., Korea Institute of Ocean Science & Technology, glyoon@kiost.ac
[2]Research Scientist, Coastal Engineering & Ocean Energy Research Dept., Korea Institute of Ocean Science & Technology, ksb9677@kiost.ac
[3]Senior Researcher, Technology Research Dept., Sambu Engineering & Construction Co. Seoul, Korea, hykim74@sambu.co.kr

ABSTRACT: One of popular offshore wind turbine foundations, monopile has been largely used because of their cheapness and constructability. Monopile is subjected by large cyclic lateral loadings such as wind, wave and current. The P-y curve method which represents a relationship between lateral pile displacement and passive soil resistance along the leading face of the pile is known as a highly reasonable method to analyses lateral behaviors of pile. Performing reliability analysis of a monopile foundation using nonlinear p-y curves is difficult because the limit state functions (LSF) of pile head deformation and rotation angle of pile are in implicit forms. To solve such problem with implicit LSF, a response surface method (RSM) could be used. Basic concept of RSM is to approximate the limit state boundary using an explicit function of the random variables. In case of using RSM, reliability analysis could be very simple, but the accuracy of analysis due to approximation depends much on the linearity of the LSF and on the distance of the axial points in the failure space. This paper investigates the best combinations of the RSM techniques with a reliability analysis of monopile for an offshore wind foundation.

INTRODUCTION

There have been developed various types of foundations for an offshore wind turbines (OWT), including gravity-typed structure, monopile, jacket, tripods and suction bucket types. Among those types of foundations, monopile is the most popular for OWT, accounting for over 75% of existing OWT foundations, by reason that those have been the most economic alternative due to their competitive fabrication and installation costs coupled with the relatively shallow-water depths at existing sites (Doherty and Gavin, 2011).

One of the well known techniques used in practice to analyze pile behaviors under lateral loadings is to model the pile as a vertical beam supported by a set of springs. The discrete springs represent the soil medium surrounding the pile. Each discrete spring is assumed to have its own load-displacement characteristic. Monopile foundation is typically designed using the p-y method for analysis of the soil-structure interaction, which varies according to soil properties, pile dimension, depth, etc. However, due to the inherent uncertainties in nature, it is difficult to determine the load-displacement characteristics of the p-y curves with depth precisely.

Geotechnical engineers have used factors of safety approach to evaluate the performance of geotechnical structures including pile foundation. The factor of safety obtained in a deterministic manner does not explicitly account for the uncertainties of load and resistance. Uncertainties of soil properties could arise because of limited site investigations, inherent variability of soil and inaccurate formula for correlating various soil parameters. Also uncertainties of the load systems, such as wind and wave, naturally occur due to different consideration in determining design loads of the pile. Because of such uncertainties, there is necessary to adopt a probabilistic approach in pile analysis.

Two aspects of interest when designing a laterally loaded pile are the lateral pile head displacement and rotational angle from the viewpoint of serviceability limit state for the stability of the whole OWT structure. Good performance of the pile will be achieved if these two aspects are satisfied. In this case, limit state function (LSF) for a lateral displacement or rotational angle of pile head become non-closed form formula. Generally it is expressed as implicit function of random variables. Therefore, reliability analysis of OWT monopile with implicit LSF, a response surface method (RSM) could be used. The basic concept of RSM is to approximate the limit state boundary by an explicit function of the random variables. In case of using RSM, reliability analysis is to be very simple, but the accuracy of analysis due to approximation depends on the linearity of the LSF and on the distance of the axial points.

This paper investigates the best combination of the RSM techniques for the reliability analysis of monopile for an offshore wind turbine foundation which have conditions at the test-bed in West-South coastal zone of Buan-Yeongkang located in Yellow Sea of Korea.

PROBABILISTIC ANALYSIS METHOD

Reliability analysis has been applied to structural design and safety reassessment of the existing structures. The probability density function of the values of the performance function can be estimated by carrying out reliability analysis using the Monte Carlo simulation (MCS) and the first-second-order reliability methods (FORM/SORM).

MCS is a numerical process to evaluate the performance function through repeated calculation based on a large number of realizations of the random variables defining the function. A MCS starts with the generation of random numbers with respective prescribed probability distributions. Methods for generating a set of random numbers with well-known distributions are widely available. The accuracy of the probability of failure obtained through MCS will improve with the sample size which is number of random numbers generated for each distribution. The ordinary Monte Carlo method can be prohibitively costly for cases with very small failure probabilities, and where the deterministic analysis for each simulation trial is computationally intensive.

Reliability index approach is one of the most reliable computational methods for structural reliability. Practical difficulty or unnecessary hardship in computing probability of failure directly has led to the development of various approximation methods, of which the first-order reliability method (FORM) is considered to one of the most reliable computational methods. FORM is an analytical approximation in which the reliability index is interpreted as the minimum distance from the origin to the limit state surface in standardized normal space and the most probable failure point (MPFP, design point) is searched using mathematical methods.

RESPONSE SURFACE METHODOLOGY

The FORM generally demands the values and partial derivatives of the LSF with respect to the design random variables. Such calculations can be performed efficiently when the LSF *g(x')* can be expressed in an explicit form or simple analytical form in terms of the design random variables *x'*. However, when the LSF is implicit, such calculations require additional efforts. A few approaches have been developed to cope with the problems with implicit LSF. One of the popular approaches is the response surface method (RSM). Response surface is the derived virtual surface which can be represented by the function of random variables. The surface is found by regression with limited responses from structural analysis and expressed in an explicit function of random variables. Then FORM is easily applied by using approximate response surface function. LSF in implicit form can be written as

$$g(X) = R(X_1, X_2, \cdots, X_n) - S(X_1, X_2, \cdots, X_n) \tag{1}$$

where R is the resistance, S is the loading function and X_i is the random variable.

First/Second order approximation of Eq. (1) can be expressed as

$$g'(X) = c_0 + c_1 X_1 + \cdots + c_n X_n \tag{2}$$

$$g''(X) = c_0 + \sum_{i=1}^{k} c_i X_i + \sum_{i=1}^{k} c_{ii} X_i^2 + \sum_{i<j} c_{ij} X_i X_j \tag{3}$$

where C_i is regression coefficient estimated by using structural responses.

The approximated function *g'(X)* is a first-order model, when the response is a linear function of independent variables. When there is a curvature in the response surface, the first-order model is insufficient. A second-order model is useful in approximating a portion of the true response surface. The second-order model includes all the terms in the first-order model, plus all quadratic terms like $c_{ii}X_i^2$ and all cross product terms like $c_{ij}X_iX_j$.

It is important to select sampling points for the accuracy of approximation of response surface. There are many designs available for fitting a second-order model. The most popular one is the central composite design (CCD) and the other one is the Bucher-Bourgunnd (B-B) method. The CCD involves 2k the axial points, 2^k factorial points and 1 central point. While B-B method involves only the axial points and central point but not cross term of factorial points.

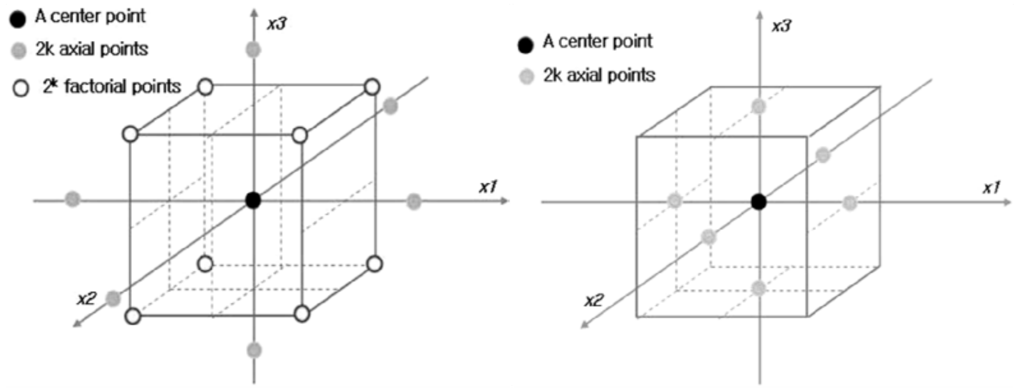

(a) Central Composite Design(CCD) (b) Bucher-Bourgunnd(B-B) method

FIG. 1. Experimental designs for fitting response surfaces.

In these method, sampling points to evaluate the coefficients C_0, C_i, C_{ij} are possible combinations of X_i's. The sampling points are selected to be located at $\mu \pm f \cdot \sigma$, where μ and σ are, respectively, the mean and the standard deviation and f is the axis point distance, which is the parameter determining the upper and lower limits of selection range.

The probabilistic characteristics of the original limit state may not be properly represented by the response surface function evaluated using the information obtained at the sampling points chosen in the vicinity of the mean values of basic random variables. To improve the accuracy of the response surface method, Bucher and Bourgunnd (1990) suggested an alternative process of selecting the sampling points. In the first step of this algorithm, the mean vector is selected as the center point. Then the response surface obtained is used to find an estimate of the design point, X_D on the interpolated limit state. In the next step, the new center point is chosen on a straight line from the mean vector μ_X to X_D so that $g(x)=0$ at the new center point, X_M , from linear interpolation, i.e.,

$$X_M = \mu_X + (X_D - \mu_X)\frac{g(\mu_X)}{g(\mu_X) - g(X_D)} \tag{4}$$

This process is assumed to guarantee that the sampling points chosen from the new center point include the information from the original failure surface sufficiently. This method is also called the adaptive response surface method.

RELIABILITY ANALYSIS OF MONOPILE

This paper focuses on preliminary design of OWT foundation at the test-bed site of Buan-Yeongkang sea located in the Yellow Sea of Korea. Offshore wind turbine NREL 5.0MW OWT monopile type is referred for a comparison as shown in Fig. 2, which has a hub height of approximately 87.6m and water depth of 15.0 m (Table 1). The combined load calculations at seabed is based on DLCs 1.3, 1.4 and 6.2 of IEC 61400-3 standard (Table 2). Ground conditions are shown in Table 3. Geotechnical investigations performed at the test bed include unconfined compression tests, triaxial compression tests and cone penetration test. Table 3 also shows that material properties of seabed soil are for a total stress analysis, given the seabed soil is consists of low permeable clay layer, which are used for estimating t-z, q-z and p-y curves to model soil-pile interaction. In this paper, t-z and q-z curves are based on API (2005), and p-y curves are based on API (2005) and Evans & Duncan (1992) to clay and sand layers, respectively.

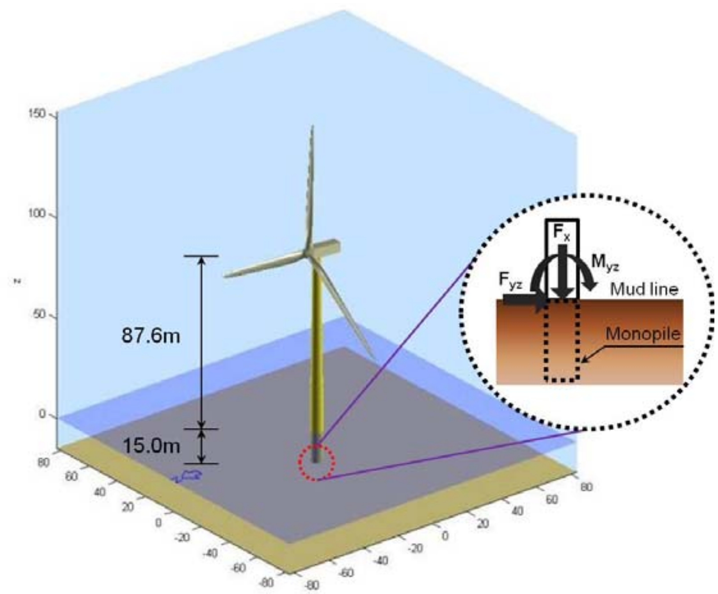

FIG. 2. A 5 MW monopile type OWT.

Table 1. Dimensions of the reference OWT

Category	Turbine	Hub height (m)	Water depth (m)
Dimensions	NREL 5.0MW	87.6	15.0

Table 2. The combined loads at seabed

Category	F_x (kN)	F_{yz} (kN)	M_{yz} (kN·m)
Combined load	11,525.0	1,676.9	168,507.0

Table 3. Ground conditions and material properties of seabed soils

Soil layer		Depth (m)	Thickness (m)	Unit weight (kN/m^3)	Cohesion (kPa)	Internal friction angle (°)
Clay	CH	0~5.0	5.0	17.0	20.00	-
	CL (1)	5.0~12.3	7.3	18.0	33.54	-
Sand	SM	12.3~23.0	10.7	19.0	16.63	31.59
Clay	CL (2)	23.0~30.0	17.0	18.0	60.00	-

It is important to quantify the uncertainty of loads (gravity, actions etc) and resistance (materials strength etc) in probabilistic analysis. Among of them, probability distribution and variability of random variables are the factors mainly affecting analysis results. In this paper, cohesion (or undrained shear strength) and internal friction angle, which are strength parameters of seabed soils, are defined as random variables. Those are normally distributed and coefficients of variance (COVs) are estimated with 0.26 (26%) and 0.063 (6.3%) to cohesion and internal friction angle, respectively, based on statistical analysis from site investigation report (Yoon et al., 2013).

Monopile foundation dimensions such as pile diameters, thickness and embeded pile length are determined reasonably through a preliminary analysis based on the above described conditions. Table 4 shows dimensions for two types of steel monopile which are to be over 3.0 of target reliability index in terms of pile diameter 6.0 m and 7.0 m. The pile is modeled by beam elements with Young's modulus of 2.1×10^8 kPa and unit weight 77 kN/m^3. And element size is specified to be 0.1m.

Table 4. Monopile foundation dimensions

Category	Case 1	Case 2	Remarks
Pile dimension (m)	6.0	7.0	steel pile
Pile wall thickness (mm)	60.0	30.0	
Embeded pile length (m)	21.6	22.5	embedded in sand

Generally in the serviceability limit state design for the stability of the whole OWT structure under lateral loads such as wind, wave and current etc, it shall be ensured that lateral deflection and rotational angle tolerances should not be exceeded. Accordingly, the major failure modes of monopile are considered as the lateral pile head displacement and rotational angle, and LSFs can be expressed as follows

$$g_1 = \delta_a - \delta_{\max}(c_{u1}, c_{u2}, c_3, \phi_3) \tag{5}$$

$$g_2 = \theta_a - \theta_{\max}(c_{u1}, c_{u2}, c_3, \phi_3) \tag{6}$$

where δ_a and θ_a are the allowable lateral displacement and rotations of the pile head; $\delta_{\max}$ and $\theta_{\max}$ are the lateral pile head displacement and rotational angle; c_{u1} is the undrained shear strength of clay_CH layer; c_{u2} is the undrained shear strength of clay_CL(1) layer; c_3 and ϕ_3 are the cohesion and internal friction angle of sand_SM layer.

$\delta_{\max}$ and $\theta_{\max}$ are performance functions of random variables such as c_{u1}, c_{u2}, c_3 and ϕ_3 by numerical investigation results. δ_a and θ_a are considered as 1% of pile diameter and 0.3 degrees respectively (DNV, 2007; Kuo et al., 2008).

To convert Eq. (5) and (6) to explicit one, g_1 and g_2 are expressed as a function of design random variables as follows

$$\begin{aligned} g_1' = {} & C_0 + C_1 c_{u1} + C_2 c_{u2} + C_3 c_3 + C_4 \phi_3 + C_5 c_{u1}^2 + C_6 c_{u2}^2 + C_7 c_3^2 + C_8 \phi_3^2 \\ & + C_9 c_{u1} c_{u2} + C_{10} c_{u1} c_3 + C_{11} c_{u1} \phi_3 + C_{12} c_{u2} c_3 + C_{13} c_{u2} \phi_3 + C_{14} c_3 \phi_3 \\ & + C_{15} c_{u1} c_{u2} c_3 + C_{16} c_{u1} c_{u2} \phi_3 + C_{17} c_{u1} \phi_3 + C_{18} c_{u2} c_3 \phi_3 + C_{19} c_{u1} c_{u2} c_3 \phi_3 \end{aligned} \quad (7)$$

$$\begin{aligned} g_2' = {} & C_0' + C_1' c_{u1} + C_2' c_{u2} + C_3' c_3 + C_4' \phi_3 + C_5' c_{u1}^2 + C_6' c_{u2}^2 + C_7' c_3^2 + C_8' \phi_3^2 \\ & + C_9' c_{u1} c_{u2} + C_{10}' c_{u1} c_3 + C_{11}' c_{u1} \phi_3 + C_{12}' c_{u2} c_3 + C_{13}' c_{u2} \phi_3 + C_{14}' c_3 \phi_3 \\ & + C_{15}' c_{u1} c_{u2} c_3 + C_{16}' c_{u1} c_{u2} \phi_3 + C_{17}' c_{u1} \phi_3 + C_{18}' c_{u2} c_3 \phi_3 + C_{19}' c_{u1} c_{u2} c_3 \phi_3 \end{aligned} \quad (8)$$

where g_1' and g_2' are approximated functions of LSFs; C_i and C_i' are the regression coefficients of response surface to be estimated from structural analysis.

Reliability analyses were conducted using in-house reliability program the HSRBD developed in KIOST (2011). To illustrate the applicability of RSM to reliability analysis, CCD and B-B method are used to formulate LSFs. Subsequently, adaptive response surface method is used to obtain optimized approximated functions. In which the initial axis point distance, $k_{initial}$, are ranging from 2 to 5. And FORM is used for the calculation of reliability index values. Finally reliability indices by the above RSM-FORM are compared with Monte Carlo simulation results for the purpose of verification. Monte Carlo simulations with 50,000 trials were carried out for each LSF, in which output sample variance of LSF is within 0.01%.

Table 5 shows lateral displacements and rotational angles of pile head and the corresponding reliability indices by MCS with failure mode in terms of each case. It is shown, in the case 1, horizontal deflections are critical failure mode, but in the case 2, rotational angles are critical failure mode.

Table 5. Reliability index with two failure modes

Category	Failure mode	Lateral Disp. (mm)		Rotation angle (°)		Reliability index (β)
		Computed	Allowable	Computed	Allowable	
Case 1	Lateral Disp.	50.5	60.0	-	-	3.35
	Rotation angle	-	-	0.252	0.3	4.53
Case 2	Lateral Disp.	51.7	70.0	-	-	5.90
	Rotation angle	-	-	0.273	0.3	3.63